Proc. Natl. Acad. Sci. USA
Vol. 88, pp. 9558–9562, November 1991
Biochemistry

The molecular structure of wild-type and a mutant Fis protein: Relationship between mutational changes and recombinational enhancer function or DNA binding

(DNA–protein recognition/structural consensus/protein crystal structure/mutations and protein conformation)

HANNA S. YUAN*, STEVEN E. FINKEL†, JIN-AN FENG*, MARIA KACZOR-GRZESKOWIAK*, REID C. JOHNSON†, AND RICHARD E. DICKERSON*

*Molecular Biology Institute and †Department of Biological Chemistry, University of California, Los Angeles, CA 90024

Contributed by Richard E. Dickerson, July 19, 1991

ABSTRACT **The 98-amino acid Fis protein from *Escherichia coli* functions in a variety of reactions, including promotion of Hin-mediated site-specific DNA inversion when bound to an enhancer sequence. It is unique among site-specific DNA-binding proteins in that it binds to a large number of different DNA sequences, for which a consensus sequence is difficult to establish. X-ray crystal structure analyses have been carried out at 2.3 Å resolution for wild-type Fis and for an Arg-89 → Cys mutant that does not stimulate DNA inversion. Each monomer of the Fis dimer has four α-helices, A–D; the first 19 residues are disordered in the crystal. The end of each C helix is hydrogen bonded to the beginning of helix B′ from the opposite subunit in what effectively is one long continuous, although bent, helix. The four helices, C, B′, C′, and B, together define a platform through the center of the Fis molecule: helices A and A′ are believed to be involved with Hin recombinase on one side, and helices D and D′ interact with DNA lying on the other side of the platform. Helices C and D of each subunit comprise a helix–turn–helix (HTH) DNA-binding element. The spacing of these two HTH elements in the dimer, 25 Å, is too short to allow insertion into adjacent major grooves of a straight B-DNA helix. However, bending the DNA at discrete points, to an overall radius of curvature of 62 Å, allows efficient docking of a B-DNA helix with the Fis molecule. The proposed complex explains the experimentally observed patterns of methylation protection and DNase I cleavage hypersensitivity. The x-ray structure accounts for the effects of mutations in the Fis sequence. Those that affect DNA inversion but not DNA binding are located within the N-terminal disordered region and helix A. This inversion activation domain is physically separated in the Fis molecule from the HTH elements and may specify a region of contact with the Hin recombinase. In contrast, mutations that affect HTH helices C and D, or interactions of these with helix B, have the additional effect of decreasing or eliminating binding to DNA.**

Fis is an *Escherichia coli* site-specific DNA-binding protein with two identical 98-amino acid subunits (Fig. 1) that functions as a regulator of many different reactions. Fis originally was identified because of its role in stimulation of the site-specific DNA inversion catalyzed by the Hin family of recombinases (1, 2). It also is involved in site-specific recombination of bacteriophage λ (3–5), *oriC*-directed DNA replication (M. Filutowicz and R. Gourse, personal communication), and transcriptional activation of several rRNA and tRNA operons (6, 7).

The mechanisms by which Fis functions in these different reactions are not known. Fis stimulation of DNA inversion has been studied extensively, and in this role, Fis activity is mediated by binding to two specific DNA sites within a recombinational enhancer sequence (8). This enhancer DNA segment functions in an orientation-independent manner from almost any location in cis relative to the recombination sites and stimulates the rate of inversion more than 100-fold (9, 10). An intermediate nucleoprotein complex formed during Hin-mediated DNA inversion, the invertasome, consists of two DNA recombination sites, the enhancer DNA, and two proteins: Fis and Hin (see figure 1 of ref. 11). Fis can be crosslinked chemically to the Hin recombinase in this complex, demonstrating the close physical proximity of the two proteins (11). It has been proposed that the C-terminal region of Fis is responsible for DNA binding, whereas an N-terminal domain interacts with Hin or in some other manner promotes inversion (12).

The DNA sequence determinants of a Fis binding site have not been precisely defined. Fis is remarkable among sequence-specific DNA-binding proteins in that it binds to so many different sequences (13, 14) and yet does not bind to other sequences that superficially appear less different from the binding sequences than those sequences do from one another. A highly degenerate "consensus" sequence has been proposed (14, 15): (G/T)NN(T/C)(A/G)NN(A/T)NN-(T/C)(A/G)NN(C/A), where N = any base. While a large number of DNA sequences that satisfy this consensus do bind Fis, many other sequences fitting this consensus do not (R.C.J., unpublished results). Polyacrylamide gel electrophoresis of Fis–DNA complexes indicates that Fis strongly bends DNA upon binding (16–18). This bending is thought to be critical for Fis activity in promoting both DNA inversion and phage λ excision (3, 12, 17). The ability of a particular DNA sequence to accept Fis-induced deformations may be important for successful binding.

It seems likely that the Fis protein is recognizing and binding to a DNA consensus *structure*, rather than a consensus sequence. One needs to know whether several DNA sequences, when bound to the Fis protein, would exhibit structural similarities that are not apparent from examination of their base sequences alone. This is one of the main goals that motivates our Fis crystal studies. Another is an understanding of how Fis mediates its various biological activities and how mutations exert their observed effects on Fis activity. As a first step in this process, we have determined the three-dimensional crystal structure of wild-type Fis and of a mutant in which amino acid Arg-89 is replaced by Cys (R89C).‡ This R89C mutant no longer binds DNA or stimulates Hin-mediated DNA inversion but is still capable of

The publication costs of this article were defrayed in part by page charge payment. This article must therefore be hereby marked "*advertisement*" in accordance with 18 U.S.C. §1734 solely to indicate this fact.

Abbreviation: HTH, helix–turn–helix.

‡The atomic coordinates for native and mutant Fis have been deposited in the Protein Data Bank, Chemistry Department, Brookhaven National Laboratory, Upton, NY 11973 (references 1FIS, 2FIS).

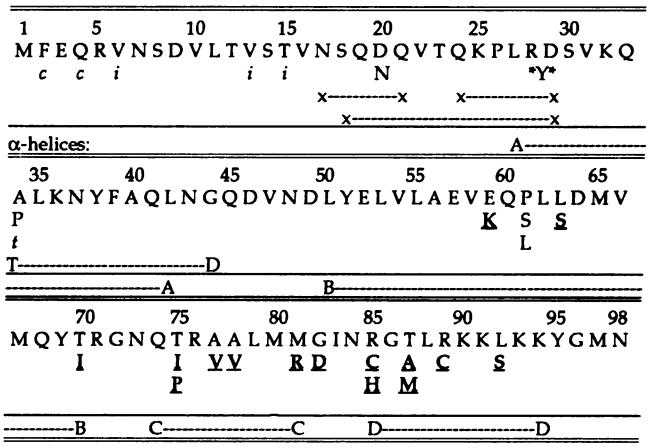

FIG. 1. Amino acid sequence, mutations, and helical regions of the *E. coli* Fis protein. The native, or wild-type, sequence is shown, with mutations listed below. x- - - -x, deletion; *Y*, insertion. Designation of phenotypes of mutations: lowercase italic, retains both Hin inversion and enhancer DNA binding; uppercase roman, inversion ineffective, but still binds to enhancer DNA; uppercase underlined boldface, neither inversion nor enhancer DNA binding. Regions of α-helices A–D from the x-ray structure analysis are indicated below the solid line.

promoting bacteriophage λ excision (12). The structure of the wild-type Fis molecule has been solved independently by Kostrewa *et al.* (18).

STRUCTURE DETERMINATION AND REFINEMENT

Large-scale purification of wild-type Fis and its R89C mutant will be described elsewhere. The purified protein was concentrated to 18 mg/ml in a solution containing 1 M NaCl, 20 mM Tris·HCl (pH 8.2), and 50 mM 2-mercaptoethanol for the mutant. Crystals were grown as rectangular rods by the sitting drop vapor diffusion method, with 1.3 M ammonia dibasic phosphate or PEG 400 as the precipitating agent. The structure of the R89C mutant was solved by multiple isomorphous replacement methods. Mersalyl was used with the R89C mutant protein (5.5 mM, 5 days of soaking), and $K_2Pt(NO_2)_4$ was used with the isomorphous wild-type protein. Statistics on the course of data collection and refinement are given in Table 1. The initial multiple isomorphous replacement map showed clean electron density for the entire dimer, with the exception of the N-terminal residues 1–24 of the first subunit and 101–124 of the second. The map was easily fitted with an atomic framework using FRODO (19).

The structure was refined with the program X-PLOR (20). The first cycle of simulated annealing gave an *R* factor of 25.6% for the 8.0–2.5 Å data from R89C Fis. This was followed by iterative refinement of atomic position and B factors and manual rebuilding of structure where necessary. In the weak N-terminal regions, density has been found subsequently from unaveraged difference maps for residues 20–24 and 120–124, although the side chains of Gln-24 and Gln-124 are missing, and a 1 Å gap exists between residues 24 and 25. A superposition of the 79 C-terminal α-carbon positions of the two independent subunits reveals only minor conformational differences: rms deviations of 0.52 Å, with the greatest deviation, as would be expected, occurring in the loop regions.

Because wild-type Fis protein is isomorphous with the R89C mutant, the mutant structure could be used as an initial model for refining the wild-type protein, with deletion of the Cys-89 and Cys-189 side chains and all water molecules. Difference Fourier maps and omit-maps showed the Arg-89 and Arg-189 side chains clearly. Subsequent refinement and search for solvent molecules were carried out as with the R89C mutant. The 79 C-terminal α-carbon atoms of native and mutant Fis show rms differences in position of only 0.18 Å.

Table 1. Crystal and refinement statistics

Parameter	Parent R89C	Parent wt	Heavy atoms Hg (R89C)	Heavy atoms Pt (wt)
Data collection				
Cell dimension, Å				
a	79.3	79.4		
b	50.5	50.9		
c	47.1	47.1		
Resolution, Å	2.3	2.25	2.5	2.5
No. of reflections				
Measured	16,603	30,267	22,806	9,112
Unique	6,184	6,451	5,666	4,453
% complete				
To 3 Å	91	89	92	88
To data limit	68	68	82	63
R_{sym}	3.92	3.23	3.73	2.84
Refinement (resolution limits 8.0–2.3 Å)				
R factor, %	18.5	18.3		
$F_o > 2\sigma$	5,913	6,053		
No. of atoms	1,284	1,291		
No. of waters	32	29		
rms errors in bonds				
Lengths, Å	0.019	0.017		
Angles, °	3.80	3.60		

The space group is $P2_12_12$, with two monomers per asymmetric unit. Hg, Mersalyl; Pt, $K_2Pt(NO_2)_4$; wt, wild type; R_{sym}, $\Sigma|\Delta F|/\Sigma F_{ave}$, where ΔF is the difference between two symmetry-related intensity observations and F_{ave} is the mean; R_{iso}, $\Sigma|F_{deriv} - F_{native}|/\Sigma F_{native}$; F_h, heavy atom structure factor; *E*, residual lack of closure; R_{Cullis}, $\Sigma|F_{h(obs)} - F_{h(calc)}|/\Sigma F_{h(obs)}$.

RESULTS

Each monomer subunit of a Fis dimer contains four α-helices: A (residues 27–42), B (50–70), C (74–81), and D (85–94), arranged as shown in Fig. 2. The first 19 residues are not visible in the electron density map, a feature that also was encountered in the analysis of Kostrewa *et al.* (18). We assume that these invisible residues are simply disordered in the crystal, since dissolved crystals yield protein that is fully active in promoting Hin-mediated DNA inversion and migrates as full length on SDS/PAGE. Beyond this initial disordered region, the electron density for each subunit is well defined. The two monomers associate by interdigitating their A and B helices, to build a compact ellipsoid with overall dimensions of about 25 × 35 × 50 Å. Each of the two long helices B that cross in the center of the dimer makes extensive van der Waals contacts and hydrogen bonds with helix A′ of the opposite monomer. Helix A has no contacts with helices C and D, which build a helix-turn-helix (HTH) structure at the bottom of the dimer as viewed in Fig. 2. Each long helix B is bent at its center toward its own HTH element, by a Pro at residue 61. This 16° bend in the overall helix B axis recalls a bend at Gly-52 in helix C of the Trp repressor (21).

The long central B helices not only help connect the two chains of the dimer but also interact with their helices C and D to establish the position and orientation of the two HTH motifs. Four main chain hydrogen bonds connect the C terminus of helix C with the N terminus of helix B′ of the opposite subunit, in a manner that virtually joins them into a bent but continuous helix, with CO-to-NH bonds: Met-80···Asp-149 (3.3 Å), Met-80···Leu-150 (3.1 Å), Met-81···Leu-150 (3.5 Å), and Met-81···Tyr-151 (3.2 Å). This simulation of a continuous helix with backbone chains that are not in fact

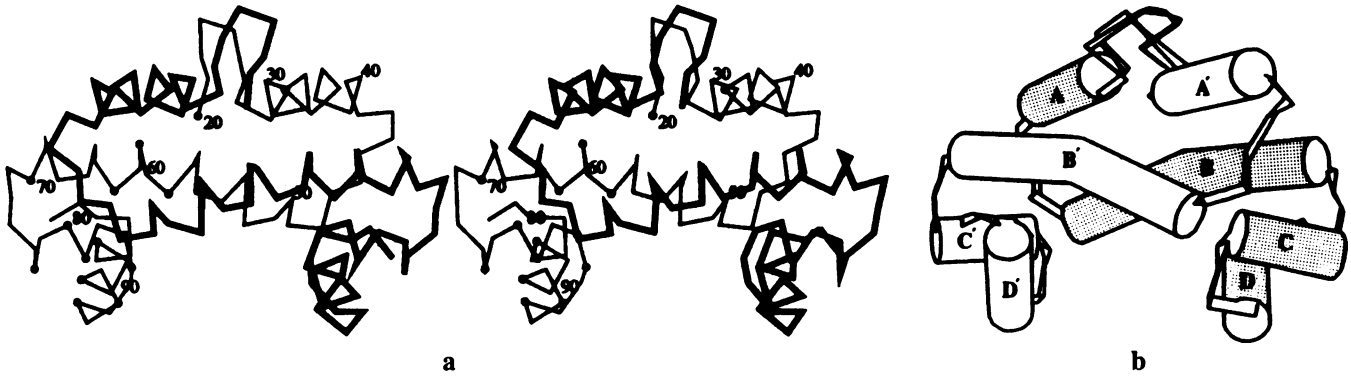

FIG. 2. (*a*) Stereopair drawing of the polypeptide chain backbone in the wild-type Fis dimer. The R89C mutant is virtually identical. Each sharp bend in the backbone chain marks an α-carbon position. Every 10th α-carbon atom from 20 to 98 is numbered in the light-line monomer, and positions of mutations listed in Fig. 1 are given by black dots. Equivalent residues in the dark-line monomer are numbered 120–198. (*b*) α-Helix cylinder diagram from the same orientation. Each helix C is in effect an extension of helix B′ of the opposite subunit. Helices C and D build HTH motifs, similar to those of other bacterial DNA-binding proteins. The Fis molecule essentially has three layers: a helix B′–C–B–C′ "ring" platform, with the helices A and A′ that are involved in promoting DNA inversion located above, and helices D and D′ that interact with DNA located below, as viewed here.

continuous is reminiscent of the stacked A-RNA helices in the D arm and anticodon arm, or the T arm and amino acid arm, of tRNA (22). Helix B also makes side chain hydrogen bonds with residues in the same-subunit helix D—Glu-52···Lys-94, Glu-59···Tyr-95, and Glu-59···Lys-91—and to helices B′ and D′ in the opposite subunit—Tyr-51···Glu-159 and Tyr-51···Lys-191. These side chain bonds are displayed as dotted lines in Fig. 3, which is a view of helices B–C–D of the Fis dimer as they would be seen by the approaching DNA.

Residues 74–94, containing helices C and D, form a HTH DNA-binding motif that resembles the HTH domains of several other bacterial DNA-binding proteins (23, 24). The amino acid sequences from several DNA-binding proteins are compared in figure 1 of ref. 24. Superposition of α-carbon positions in this 20-residue HTH region yields a rms difference of only 0.44 Å between Fis and phage λ cro and 0.47 Å between Fis and phage 434 cro. Residues at positions 4, 8, 10, 15, and 18 within each HTH element usually are hydrophobic and define the interior of the elbow between helices. These residues in Fis are Ala-77, Met-81, Ile-83, Leu-88, and Lys-91. The anomalously hydrophilic Lys-91 of Fis lies on the surface and forms the previously mentioned hydrogen bonds with Glu-59 in the B helix and Tyr-151 in the B′ helix of the opposite chain (Fig. 3), thus helping to knit the Fis dimer together. Close steric contacts require a Gly or Ala (Ala-78 in Fis) at position 5 in almost all known examples of the HTH motif. Similarly, the residue at HTH position 9 is usually a Gly (Gly-82 in Fis), most probably because only Gly can accommodate the ϕ and ψ angles needed for the sharp turn between helices.

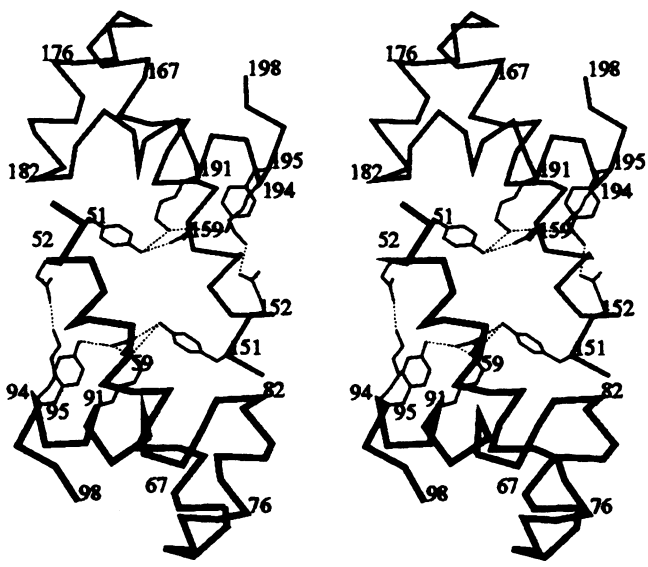

FIG. 3. Stereoview of the B, C, and D helices of both monomers, as seen from the direction of an approaching DNA helix. The main chain is represented only by straight lines between α-carbon atoms. Side chains shown are those whose hydrogen bonds help hold these helices in a fixed geometry. The ring platform built by helices B′–C–B–C′ lies in the plane of the page; DNA-binding D helices in front and invertasome-interacting A helices behind the platform have been omitted for clarity.

The overall appearance of the Fis dimer in Fig. 2 suggests that helix D inserts into the DNA major groove. If so, then the polar and generally positively charged residues Arg-85, Thr-87, Arg-89 (Cys-89 in the mutant Fis), Lys-90, and Lys-93 most likely contact the phosphate backbone or the floor of the major groove. The loss of a positive charge at position 89 may explain why the R89C mutant binds less well to the λ site and not at all to the Hin enhancer binding sites.

DISCUSSION

Modeling a Fis–DNA Complex. The common pattern in other HTH proteins is for two HTH motifs of a dimer to be separated by a distance such that they can be inserted into adjacent major grooves of the DNA. If measured at phosphates on the helix surface, the major groove in B-DNA makes an angle of ≈32° with a plane normal to the helix axis. The distance from one major groove to the next along the helix axis is 34 Å, and so the shortest distance between centers of adjacent major grooves is 34 cos(32°) = 29 Å. In Fis the two D helices are oriented as though they are to be fitted into two adjacent major grooves but are only 25 Å apart. A rigid Fis molecule will not fit onto a rigid DNA helix. But since Fis is known to bend DNA upon binding (12, 14, 15), a strong inference is that Fis must bend the DNA in a manner that reduces the distance between adjacent major grooves. Kostrewa *et al.* (18) came to the same conclusion for similar reasons.

We have constructed a preliminary model for a Fis–DNA complex by "docking" the Fis structure with a bent molecular model of the Hin enhancer distal Fis-binding sequence. The model maximizes the number of hydrogen bonds that can be formed between the HTH domain and DNA and was refined by X-PLOR to minimize energy. The nucleotide se-

quence of the Hin enhancer site to which Fis was modeled is

```
 1          9          18          27
5'-TTACTA|GTG|CAAA|T|TGTG|ACC|GCATTT
        a   b    c c    b   a
3'-AATGAT|CAC|GTTT|A|ACAC|TGG|CGTAAA
  54         45         36         28
```

The 15-base-pair "core" binding site is located between nucleotides 7 and 21 and nucleotides 34 and 48, or from "a" to "a" above. Underlined G residues represent those nucleotides in adjacent major grooves that are protected from dimethyl sulfate modification and that prevent Fis binding when methylated at their N-7 position. Base pair steps marked "a" and "b" above are sites that are hypersensitive to DNase I cleavage when the double helix is bound to Fis (8). These positions are represented by yellow and red highlighted bases, respectively, in the model shown in Fig. 4.

Suck *et al.* (25) have suggested that DNase I digestion hypersensitive sites in DNA–protein complexes might occur at sites where the minor groove is expanded by bending of the helix. The Fis sequence above was bent by introducing roll angles of +10° at steps "a" and of +15° at steps "b". Steps "c" near the center were each given −20° roll, locally compressing the minor groove. Because steps "b" and "c" are a half turn of helix apart, their positive and negative rolls reinforce, to create the strong curvature in helix visible in Fig. 4. These rolls give the DNA segment a net bending radius of ≈62 Å and an overall bend angle of 59°. Whereas various Fis-induced bend angles are measured in solution at different binding sites, a bending angle of 59° is similar to the value measured at the Hin enhancer distal site using the method of Thompson and Landy (ref. 16; and A. Glasgow, M. I. Simon, and R.C.J., unpublished results). Rigid body energy minimization, including positively charged and other side chains on C and D helices, led to a final model (Fig. 4) that is consistent with many of the known properties of the complex. Extensive interaction is obtained between positive side chains and the phosphate backbone of the helix. Especially close contacts are observed between Fis side chains and the five purines—G7, G18, G34, G35, and G45—that are known to be protected from methylation by binding of Fis (8). These are indicated in yellow in Fig. 4.

Structural Interpretation of Biochemical Properties of Fis Mutants. Recent genetic analysis of Fis has identified three categories of mutational changes within the protein sequence (ref. 12; see summary in Fig. 1). These include mutants that (*i*) largely retain both Hin-mediated DNA inversion activity and enhancer DNA binding, (*ii*) lose DNA inversion activity but retain DNA binding, and (*iii*) lose both DNA inversion and DNA-binding capabilities. Analysis of the Fis crystal structure suggests molecular explanations for the phenotypes of many of these mutants.

The overall properties of the N-terminal mutants of Fis indicate that at least parts of the N-terminal extended region and helix A are critical for promoting DNA inversion but are not involved directly in binding DNA or in promoting λ excision (12). The mutant data combined with the crosslinking of Fis and Hin in the invertasome complex (11) suggest that Fis bound to its recombinational enhancer may be interacting specifically with the Hin recombinase in the complex. The disordered portion of the N-terminal segment may interact with Hin and adopt a more rigid structure. Similar models have been proposed for the association of certain transcription factors upon interaction with other proteins of the transcriptional apparatus, as well as the ordering of the DNA-binding regions of leucine zipper proteins when they interact specifically with DNA (26). An alternative model is that the N-terminal segment may interact with DNA to facilitate invertasome assembly, for example by stabilizing a supercoiled node—the crossing DNA strands in the invertasome (27).

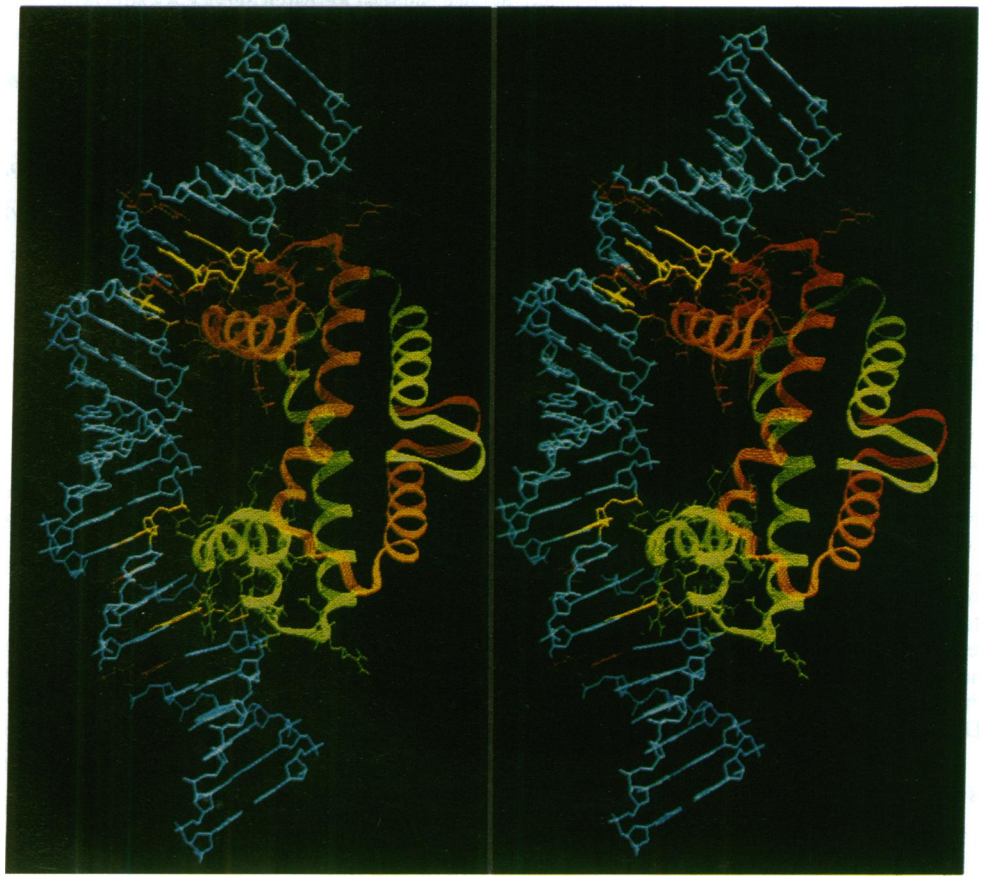

FIG. 4. Stereo drawing of the modeling of bent DNA to the Fis molecule. The two Fis chains are in orange and green; side chains are drawn only in the C–D HTH regions. Base pair T1·A54 is at the bottom, and T27·A28 is at the top. Yellow denotes the five purines that are protected against methylation by binding of Fis. Red bases in the DNA are sites that are made hypersensitive to DNase I cleavage by binding of Fis, presumably because of the bending that Fis induces in the double helix. For the method of generating this docking model, see the text.

With the two exceptions noted below (at Pro-61), all of the mutations that affect Fis stimulation of DNA inversion while retaining DNA binding are located in the N-terminal disordered region and in helix A (see Fig. 1). These include several deletions located between residues 17 and 29 that completely abolish recombinational enhancer activity. Particularly strong single amino acid substitutions with these properties are Asp-20 → Asn and Ala-34 → Pro. Both changes may affect the overall structure of the N-terminal domain, since the Asp-20 side chain is in van der Waals contact with helices A′ and B′ of the other Fis subunit, and substitution of Pro for Ala at position 34 may disrupt helix A itself. (As Fig. 1 indicates, substitution of Thr for Ala-34 is much less severe.) Mutations located nearest the N terminus, such as Phe-2 → Cys, Gln-4 → Cys, Val-6 → Ile, Val-13 → Ile, and Thr-15 → Ile, have only a modest effect on DNA inversion.

Mutations within the central helix B region of Fis display radically different phenotypes. Replacement of Pro-61 by Leu or Ser severely affects the ability of the mutant protein to promote DNA inversion but does not affect DNA binding. As shown in Fig. 2, this Pro is packed against helix A′ of the opposite subunit, in addition to its role in producing a bend in helix B itself. Substitution at this position may affect the structure of the top half of the molecule, as drawn in Fig. 2, more than the HTH motif at the bottom. Two other mutations in this same helix B region, Glu-59 → Lys and Leu-63 → Ser, abolish DNA binding even though they lie outside the HTH region of helices C and D. The reasons for this are readily apparent from the x-ray structure. As mentioned earlier, Glu-59 is part of a hydrogen-bonded network that also involves Lys-91, Tyr-95, and Tyr-151 and that holds the HTH motif in the proper configuration (Fig. 3). Loss of this network presumably allows the C and D helices to shift in a manner that is not conducive to DNA binding. Leu-63 is in van der Waals contact with residues Lys-91 and Tyr-95 in the D helix and thus is important in orienting the HTH domains.

All mutations in the HTH region, residues 70–94, reduce DNA binding to various degrees. Mutations Thr-70 → Ile, Thr-75 → Ile, and Ala-77 → Val greatly decrease the affinity of Fis for DNA without abolishing binding altogether. For each of these mutants the hydrophobicity of the side chain is increased, which probably produces local backbone conformation changes. However, introduction of a Pro into the C helix by a Thr-75 → Pro mutation is more serious, and DNA binding is eliminated. Similarly, the Ala-78 → Val mutation is more severe than Ala-77 → Val, presumably because it introduces a bulky side chain at a point of close contact between the C and D helices, thus deforming the HTH unit.

Mutations beyond residue 80 are uniformly disruptive of DNA binding. Met-81 → Arg introduces a positive charge at a contact point between helices B and C. Gly-82 → Asp eliminates the Gly that is necessary for the β turn between helices C and D. Arg-85 → Cys and Arg-85 → His mutations break a hydrogen bond to Gln-74 or Thr-75 that holds helices C and D together. Moreover, removal of a positive charge by either of these mutations or by Arg-89 → Cys probably breaks an interaction with the negatively charged DNA. Mutations Thr-87 → Ala and Thr-87 → Met both result in significant reduction of DNA binding, but the protein–DNA complexes that are formed migrate as less bent on polyacrylamide gels (12). These mutations introduce a hydrophobic patch at what our Fis–DNA docking model indicates should be a contact point between protein and DNA. Finally, substitution of a polar for a nonpolar residue by Leu-92 → Ser disrupts the hydrophobic core of the HTH element near the end of the D helix.

CONCLUSION

In summary, the x-ray crystal structure of the Fis protein suggests a model for bending and docking with DNA and provides a ready explanation for the biological effects of all of the observed mutations. To our knowledge, Fis is the first HTH protein to have its DNA recognition helices separated by significantly less than 34 Å, and this may reflect the bending of DNA that occurs when it binds to Fis. Other HTH proteins that bend DNA, such as the phage 434 repressor, Trp repressor, and cAMP binding protein, do so via kinks at the two major groove sites where the HTH units bind, with a straight helix between these sites. Limited reduction of the distance between HTH binding sites is produced by an overwinding that compresses the minor groove. Fis may achieve an even further diminution of the distance between HTH sites by introducing a bend into the minor groove at the very center of the DNA site.

Fis also is unique among site-specific DNA-binding proteins in that it binds specifically to a series of weakly related DNA sequences. Though a highly degenerate consensus sequence can be found, many sites that satisfy this consensus will not bind Fis. We suspect that this paradox reflects chiefly our lack of knowledge about the true relationships between base sequence and local helix structure and that those sequences that bind Fis well ultimately will be shown to possess a common local structure that at the moment is unpredictable. Badly needed at present are the crystal structures of the Fis protein bound to four or five different DNA sequences, if possible, of varying strengths of binding. The versatility of its binding makes Fis admirably suited to be a "laboratory" for protein–DNA binding studies.

We would like to thank Mary L. Kopka for helpful suggestions on crystallization and Chris P. Hill, Seounghyon Choe, and Duilio Cascio for advice on data analysis and refinement. Robert Osuna also has contributed valuable discussions on the analysis of mutants. This work was performed with the support of National Institutes of Health Program Project Grant GM-31299 to R.E.D. and Grant GM-38509 to R.C.J. Support was also provided to R.C.J. from the Searle Scholars Program/The Chicago Community Trust and to S.E.F. by U.S. Public Health Service National Research Service Award GM-07104.

1. Johnson, R. C., Bruist, M. F. & Simon, M. I. (1986) *Cell* **46**, 531–539.
2. Koch, C. & Kahmann, R. (1986) *J. Biol. Chem.* **261**, 15673–15678.
3. Thompson, J. F., Moitoso de Vargas, L., Koch, C., Kahmann, R. & Landy, A. (1987) *Cell* **50**, 901–908.
4. Ball, C. A. & Johnson, R. C. (1991) *J. Bacteriol.* **173**, 4027–4031.
5. Ball, C. A. & Johnson, R. C. (1991) *J. Bacteriol.* **173**, 4032–4038.
6. Nilsson, L., Vanet, A., Vijgenboom, E. & Bosch, L. (1990) *EMBO J.* **9**, 727–734.
7. Ross, W., Thompson, F., Newlands, J. T. & Gourse, R. L. (1990) *EMBO J.* **9**, 3733–3742.
8. Bruist, M. F., Glasgow, A. C., Johnson, R. C. & Simon, M. I. (1987) *Genes Dev.* **1**, 762–772.
9. Johnson, R. C. & Simon, M. I. (1985) *Cell* **41**, 781–791.
10. Kahmann, R., Rudt, F., Koch, C. & Mertens, G. (1985) *Cell* **41**, 771–780.
11. Heichman, K. A. & Johnson, R. C. (1990) *Science* **249**, 511–517.
12. Osuna, R., Finkel, S. E. & Johnson, R. C. (1991) *EMBO J.* **10**, 1593–1603.
13. Travers, A. A. (1991) *Curr. Biol.* **1**, 171–173.
14. Hübner, P. & Arber, W. (1989) *EMBO J.* **8**, 577–585.
15. Johnson, R. C., Glasgow, A. C. & Simon, M. I. (1987) *Nature (London)* **329**, 462–465.
16. Thompson, J. F. & Landy, A. (1988) *Nucleic Acids Res.* **16**, 9687–9705.
17. Hübner, P., Haffter, P., Iida, S. & Arber, W. (1989) *J. Mol. Biol.* **205**, 493–500.
18. Kostrewa, D., Granzin, J., Koch, C., Choe, H.-W., Raghunathan, S., Wolf, W., Labahn, J., Kahmann, R. & Saenger, W. (1991) *Nature (London)* **349**, 178–180.
19. Jones, T. A. (1978) *J. Appl. Crystallogr.* **11**, 268–272.
20. Brunger, A. T., Kuriyan, J. & Karplus, M. (1987) *Science* **235**, 458–460.
21. Schevitz, R. W., Otwinowski, Z., Joachimiak, A., Lawson, C. & Sigler, P. B. (1985) *Nature (London)* **317**, 782–786.
22. Kim, S.-H. (1978) *Adv. Enzymol.* **46**, 279–315.
23. Steitz, T. A. (1990) *Q. Rev. Biophys.* **23**, 205–280.
24. Harrison, S. C. & Aggarwal, A. K. (1990) *Annu. Rev. Biochem.* **59**, 933–969.
25. Suck, D., Lahm, A. & Oefner, C. (1988) *Nature (London)* **332**, 466–468.
26. Frankel, A. D. & Kim, P. S. (1991) *Cell* **65**, 717–718.
27. Kanaar, R., van de Putte, P. & Cozzarelli, N. R. (1988) *Proc. Natl. Acad. Sci. USA* **85**, 752–756.